Carbohydrate Polymers 121 (2015) 449–456

Contents lists available at ScienceDirect

Carbohydrate Polymers

journal homepage: www.elsevier.com/locate/carbpol

Structural studies of an arabinan from the stems of *Ephedra sinica* by methylation analysis and 1D and 2D NMR spectroscopy

Yong-Gang Xia [1], Jun Liang [1], Bing-You Yang, Qiu-Hong Wang, Hai-Xue Kuang*

Key Laboratory of Chinese Materia Medica (Heilongjiang University of Chinese Medicine), Ministry of Education, Harbin 150040, PR China

ARTICLE INFO

Article history:
Received 2 November 2014
Received in revised form
23 December 2014
Accepted 25 December 2014
Available online 3 January 2015

Keywords:
Ephedra sinica
Arabinan
NMR
Structural elucidation

ABSTRACT

Plant arabinan has important biological activity. In this study, a water-soluble arabinan ($M_w \sim 6.15$ kDa) isolated from the stems of *Ephedra sinica* was found to consist of (1→5)-Ara*f*, (1→3,5)-Ara*f*, T-Ara*f*, (1→3)-Ara*f* and (1→2,5)-Ara*f* residues at proportions of 10:2:3:2:1. A tentative structure was proposed by methylation analysis, nuclear magnetic resonance (NMR) spectroscopy (^{1}H NMR, ^{13}C NMR, DEPT-135, ^{1}H–^{1}H COSY, HSQC, HMBC and ROESY) and literature. The structure proposed includes a branched (1→5)-*α*-Ara*f* backbone where branching occurs at the O-2 and O-3 positions of the residues with 7.7% and 15.4% of the 1,5-linked *α*-Ara*f* substituted at the O-2 and O-3 positions. The presence of a branched structure was further observed by atomic force microscopy. This polymer was characterized as having a much longer linear (1→5)-*α*-Ara*f* backbone as a repeating unit. In particular, the presence of *α*-Ara*f*→3)-*α*-Ara*f*-(1→3)-*α*-Ara*f*-(1→ attached at the O-2 is a new finding. This study may facilitate a deeper understanding of structure–activity relationships of biological polysaccharides from the stems of *E. sinica*.

1. Introduction

Ephedra sinica Stapf, known as Ma Huang in Chinese, is a shrub used medically for centuries (Mehendale, Bauer & Yuan, 2004). *E. sinica* contains a high account of polysaccharides, which range from 3% to 5% of the total dry weight (Xia et al., 2011b). Recently, polysaccharides from *E. sinica* have been shown to have immunosuppressive effects (Kuang, Xia, Yang, Wang & Wang, 2011; Kuang et al., 2011b). Until recently, various polysaccharides from *E. sinica* have been extensively investigated, including chemical characterization and pharmacological functions widely studied in our lab (Kuang et al., 2011c; Xia et al., 2011a).

During the past decade, an impressive number of structurally diverse and biologically active arabinans have been isolated and identified from herb plants (Cardoso, Silva & Coimbra, 2002; Dourado, Cardoso, Silva, Gama & Coimbra, 2006; Mandal et al., 2011). Furthermore, arabinan and arabinan-rich pectins have been reported to possess a wide range of biological activity profiles including gastro-protective (Cordeiro et al., 2012), as well as immunological (Dourado et al., 2004; Mandal et al., 2013) and anticoagulant activities (Fernandez et al., 2013; Uehara, Takeshita & Maeda, 1992).

As part of the ongoing studies of biological polysaccharides, we isolated a water-soluble arabinan from the stem of *E. sinica* and seek to develop a carbohydrate-based drug. To date, there is no structural study on arabinan from the stem of *E. sinica*. Therefore, it is important to carry out the detailed structural research on this polysaccharide because it will elucidate its structure-bioactivity relationship, which is beneficial for the development of polysaccharides from the stems of *E. sinica*. Detailed structural studies of this arabinan molecule were carried out by methylation analysis, 1D and 2D-NMR experiments (^{1}H, ^{13}C, DEPT-135, ^{1}H–^{1}H COSY, HSQC, HMBC and ROESY) and atomic force microscopy.

2. Materials and methods

2.1. Isolation and purification of ESP-B1H from E. sinica

The ESP-B1 was isolated from the stems of *E. sinica* according to our previous procedure (Kuang et al., 2011a). Fraction ESP-B1 (120.0 mg) was further reiteratively chromatographed over Sephadex G50 eluting with distilled water to afford ESP-B1H (90.0 mg). The yield regarding the wet/dry plant mass was 0.15 mg/g for ESP-B1H.

* Corresponding author. Tel.: +86 45182193001; fax: +86 45182110803.
E-mail address: hxkuang@hotmail.com (H.-X. Kuang).
[1] These authors contributed equally to this article.

http://dx.doi.org/10.1016/j.carbpol.2014.12.058
0144-8617/

2.2. Determination of molecular weight

The molecular weight of the polysaccharide was determined by gel-permeation chromatography. Dextran standards (T-10, T-40, T-70, T-500 and T-2000) were used as a calibration curve by HPLC-ELSD on a Shodex sugar KS-805 column (8.0 mm × 300 mm, 17 μm) coupled with a Shodex KS-G guard column (6 mm × 50 mm, 7 μm). Detailed conditions have been described in our previous report (Kuang et al., 2011c).

2.3. Monosaccharide compositional analysis

The polysaccharide (3 mg) was hydrolyzed with 2 M CF_3COOH in a round bottom flask at 100 °C for 10 h in a boiling water bath. The excess acid was completely removed and co-distilled with methanol. A PMP derivative was made from the hydrolyzed product. The analysis of PMP-labeled monosaccharides was carried out on a Waters Acquity UPLC system coupled with a photodiode array detection (Kuang et al., 2011c).

2.4. Methylation analysis

The polysaccharide ESP-B1H (5 mg) was methylated three times with powdered sodium hydroxide and methyl iodide in dimethy sulphoxide solution. The methylated products were isolated by partitioning between $CHCl_3$ and H_2O (3:1, v/v). The organic layer containing products was washed with 3 mL water three times and dried. The resulting partially methylated products were hydrolyzed, reduced, acetylated and analyzed using a DSQ II GC–MS system (Thermo Fisher Scientific) with DB-5 capillary column (30 m × 0.25 mm × 0.25 μm). The oven condition was initially 80 °C during injection for 1 min. It increased at 5 °C/min to 200 °C, then 10 °C/min to 270 °C and then held at this temperature for 1 min. The partially methylated alditol acetates were identified by their relative retention times on GC and fragment ions in EI-MS, and the molar ratios were estimated from the peak areas.

2.5. Nuclear magnetic resonance (NMR) spectroscopy

The sample ESP-B1H was dissolved in D_2O to exchange the active hydrogen and was then lyophilized. This process was repeated three times. The ^1H NMR and ^{13}C NMR spectra were obtained on a Bruker DPX 400 MHz for δ_H and 100 MHz for δ_C, at room temperature (25 °C), in D_2O. The DEPT experiments were done using a polarization-transfer pulse of 135°. The ROESY mixing delay was 300 ms. The ^1H–^1H COSY, HSQC and HMBC were carried out using standard Bruker software. Chemical shifts are given as δ values with reference to tetramethylsilane (TMS) as an internal standard, and coupling constants are given in Hz.

2.6. Atomic force microscopy (AFM)

The atomic force microscopy in this study was recorded in SPI38OON atomic force microscope (Harbin Institute of Technology, Harbin, China). Atomic force microscopy used tapping mode. The ESP-B1H was diluted to a final concentration of 5.0 μg/mL in distilled water. 300 μL samples were dropped onto freshly cleaved mica and allowed to stand in air before imaging.

3. Results and discussion

3.1. Monosaccharide composition and molecular weight

Although ESP-B1 was detected as a symmetrical peak, some minor impurities were found via Sephacryl S-100 HR column chromatography (Kuang et al., 2011a). Thus, this fraction was further purified on Sephadex G-50 to yield ESP-B1H featured at high arabinofuranosyl content. The ESP-B1H appeared as a highly symmetrical and sharp peak in HPLC-ELSD with Shodex sugar KS-805 column (Fig. 1). Thus, ESP-B1H was selected for structural research on the basis of chemical and extensive spectroscopic analysis.

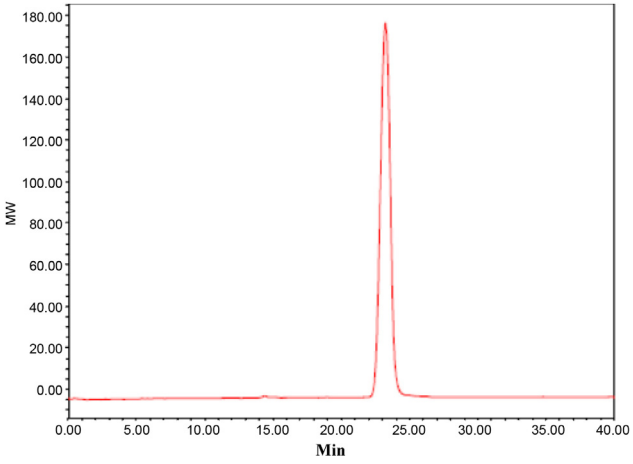

Fig. 1. HPLC-ELSD chromatogram of ESP-B1H using a Shodex sugar KS-805.

The ESP-B1H was a white, amorphous powder. The average molecular weight was 6.15 kDa using standard dextrans. The monosaccharide composition of ESP-B1H was analyzed by UPLC analysis based on pre-column derivatization with PMP reagent after full acid hydrolysis. Compared to monosaccharide standards, ESP-B1H was mainly composed of arabinose (96%) with trace amount of neutral sugars such as glucose, mannose and galactose. This indicated that ESP-B1H was an arabinan.

3.2. Methylation and GC–MS analysis

It is well-known that methylation analysis is the most commonly used method for determining the substitutional pattern of the monosaccharide units in polysaccharides (Kang et al., 2011; Yin, Lin, Nie, Cui & Xie, 2012). The preparation of partially O-methylated alditol acetates (PMAAs) involved successive methylation, hydrolysis, reduction and acetylation identified with GC–MS using EI-MS fingerprints.

As shown in Table 1, five major GC–MS chromatography peaks at 18.05, 20.28, 21.11, 22.77 and 23.08 min can be identified as 2,3,5-tri-O-methyl-1,4-di-O-acetyl-arabinitol, 2,3-di-O-methyl-1,4,5-tri-O-acetyl-arabinitol, 2-O-methyl-1,3,4,5-tri-O-acetyl-arabinitol, 3-O-methyl-1,2,4,5-tri-O-acetyl-arabinitol and 2,5-di-O-methyl-1,3,4-tri-O-acetyl-arabinitol based on characteristic EI-MS fragmentation pathways of different PMAAs, respectively. These data further indicated that all arabinosyl residues should be a furanose rather than a pyranose.

Thus, the typical glycosidic linkages of arabinosyl residues were determined to be T-Ara*f*, (1→5)-Ara*f*, (1→3,5)-Ara*f*, (1→2,5)-Ara*f* and (1→3)-Ara*f* in a molar ratio of nearly 3:10:2:1:2. The semi-qualitative results showed (1→5)-Ara*f* is the most important linkage unit and accounts for more than 55% of the residues. This result indicates this molecule includes a (1→5)-α-Ara*f* backbone where branching occurs at the O-2 and O-3 positions of the residues.

3.3. 1D and 2D NMR analysis

3.3.1. ^1H NMR analysis

The downfield chemical shifts at δ 4.9–5.2 in the ^1H NMR spectrum of ESP-B1H indicated a structural feature of common

Table 1
GC–MS data for methylation analysis of ESP-B1H.

t_R *(min)	Sugar derivative	Mode of linkage	Key mass fragments (*m*/*z*) (relative abundance, %)
18.05	2,3,5-tri-*O*-methyl-1,4-di-*O*-acetyl-arabinitol	α-Ara*f*-(1→	161 (42), 129 (80), 117 (100), 101 (48), 87 (28), 71 (18), 43 (80)
20.28	2,5-di-*O*-methyl-1,3,4-tri-*O*-acetyl-arabinitol	→3)-α-Ara*f*-(1→	233 (15), 189 (10), 129 (42), 117 (100), 87 (25), 71 (9), 43 (90)
21.11	2,3-di-*O*-methyl-1,4,5-tri-*O*-acetyl-arabinitol	→5)-α-Ara*f*-(1→	189 (25), 129 (67), 117 (100), 101 (23), 87 (30), 71 (8), 43 (61)
22.77	2-*O*-methyl-1,3,4,5-tri-*O*-acetyl-arabinitol	→3,5)-α-Ara*f*-(1→	261 (15), 201 (9), 159 (12), 127 (20), 117 (100), 99 (20), 43 (99)
23.08	3-*O*-methyl-1,2,4,5-tri-*O*-acetyl-arabinitol	→2,5)-α-Ara*f*-(1→	189 (40), 129 (100), 87 (32), 43 (39)

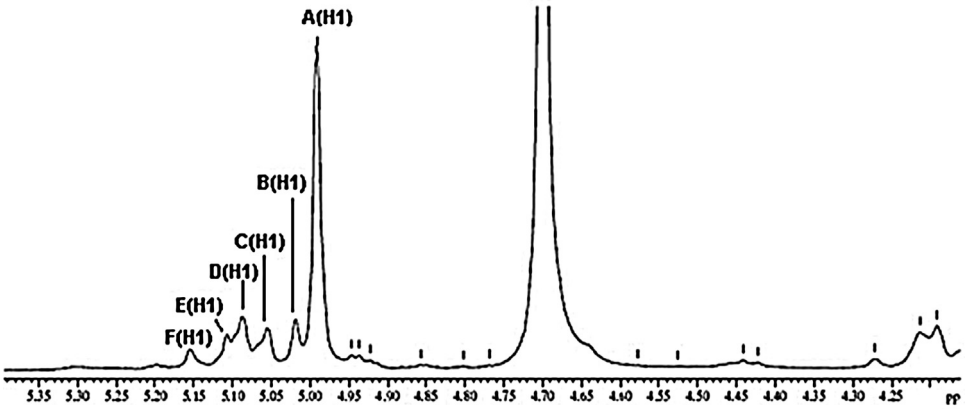

Fig. 2. Part of ^{1}H NMR spectrum of ESP-B1H.

arabinans (Dourado et al., 2006; Shakhmatov, Toukach, Michailowa & Makarova, 2014). Signals from glucose, mannose and galactose were not observed in the spectrum due to their relatively low proportions. The anomeric region in the ^{1}H NMR spectrum of ESP-B1H had six resonances that could be assigned to anomeric protons with H-1 chemical shifts of 4.99 (*br. s*), 5.02 (*br. s*), 5.06 (*br. s*), 5.09 (*br. s*), 5.10 (*br. s*) and 5.15 (*br. s*). These six obvious anomeric proton signals at δ 4.99–5.15 were described to be **A**(**H1**)-**F**(**H1**) due to their increasing anomeric proton chemical shifts (Fig. 2). According to the methylation and comparison with literature data (Cardoso et al., 2002; Dourado et al., 2006; Mandal et al., 2011; Mandal et al., 2013; Shakhmatov et al., 2014; Westphal et al., 2010), the corresponding sugar residues **A-F** were then tentatively identified as (1→5)-Ara*f*, (1→3,5)-Ara*f*, T-Ara*f*, (1→3)-Ara*f*, (1→2,5)-Ara*f* and T-Ara*f*, respectively.

In the ^{1}H NMR spectrum, integrated peak area is proportional to the number of observed ^{1}H nuclei (Muncey, Jones, De Iorio & Ebbels, 2010). This allows quantification of the sugar residues. Therefore, it is reasonable that the molar ratio of sugar residues **A-F** were calculated with their integrated peak areas of the anomeric protons in the ^{1}H-NMR spectrum. The current results indicate that the relative molar ratios of the sugar residues **A-F** were nearly 10:2:2:2:1:1. This further confirmed the GC–MS data. It showed a good correlation between the terminal and branched arabinofuranosyl residues for the low degree of polymerization of this polymer. The above data further indicated that repeating unit of ESP-B1H possesses a branched (1→5)-α-Ara*f* backbone where branching occurs at O-2 and O-3 positions of residues. Here 7.7% and 15.4% of 1,5-linked α-Ara*f* were substituted at O-2 and O-3 positions to form 1,2,5-linked and 1,3,5-linked α-Ara*f* moieties, respectively. It is well-known that coupling constants (J_{H1-H2}) of α-anomeric protons differ remarkably from that of β-oriented anomer for arabinosyl moiety (Dourado et al., 2006; Mandal et al., 2011). They can be used for the identification of the anomeric configuration of the arabinosyl residues. In this study, the J_{H1-H2} of the anomeric protons in all of the arabinosyl residues were observed as a broad singlet (*br. s*) indicating that they were present as an α-anomer.

3.3.2. ^{13}C NMR analysis

The ^{13}C NMR spectrum and DEPT-135 experiment of the polysaccharide also showed characteristic arabinosyl signals (Fig. 3). The abnormal downfield chemical shifts of anomeric carbons (δ107.5–106.4) for all the arabinosyl residues indicated that these were present as furanose and not as pyranose form (Dourado et al., 2006; Mandal et al., 2011). The anomeric carbon signals at δ 107.5–106.4 were labeled as **A(C1)-F(C1)** according to ^{1}H–^{13}C HSQC spectrum. Furthermore, the relative configuration of arabinofuranosyl was further determined as α-oriented by the characteristic downfield chemical shifts of the anomeric carbons (Cardoso et al., 2002; Mandal et al., 2011). A combination of literature data published for spectra of arabinans (Cordeiro et al., 2012; Dourado et al., 2006; Mandal et al., 2011), arabino-oligosaccharides (Westphal et al., 2010) and arabinan-rich pectins (Shakhmatov et al., 2014) allowed us to identify (1→5)-α-Ara*f* (**A**), (1→3,5)-α-Ara*f* (**B**), T-α-Ara*f* (**C**/**F**), (1→3)-α-Ara*f* (**D**) and (1→2,5)-α-Ara*f* (**E**), which concurred with methylation analysis (Tables 1 and 2).

A notable feature of ^{13}C NMR spectrum of ESP-B1H was appearance of a downfield methine carbon signal at δ 86.9 due to the C-2 of the residue **E** (Mandal et al., 2013; Navarro, Cerezo & Stortz, 2002). Also, the well-defined methylene carbon signals at δ66.8, 66.4 and 61.1 could be attributed to the C-5 of the residues **A**, **B**/**E** and **C**/**D**/**F**, respectively. Since the residues **C**, **D** and **F** are present as non-reducing terminal ends and side chains, the backbone chain of the present arabinan would have (1→5)-linked residues consisting of **A**, **B** and **E**, with (1→5), (1→3,5) and (1→2,5)-linked moieties, respectively. Residues **B** and **E** possess more rigid molecular structure than **A** (Mandal et al., 2011). Hence, **B(C5)** and **E(C5)** (δ_C 66.4) would be more shielded than **A(C5)** (δ_C 66.8). This observation was further confirmed by literature data (Mandal et al., 2013; Thude & Classen, 2005).

3.3.3. 2D NMR analysis

All hydrogen and carbon signals were assigned as much as possible through a combination of DEPT-135, ^{1}H–^{1}H COSY, HSQC, HMBC and ROESY experiments (Table 2). From ^{1}H–^{1}H COSY spectrum (Fig. 4), we correlated **A(H1)** (δ_H 4.99) and **A(H2)** (δ_H 4.03), **A(H2)**

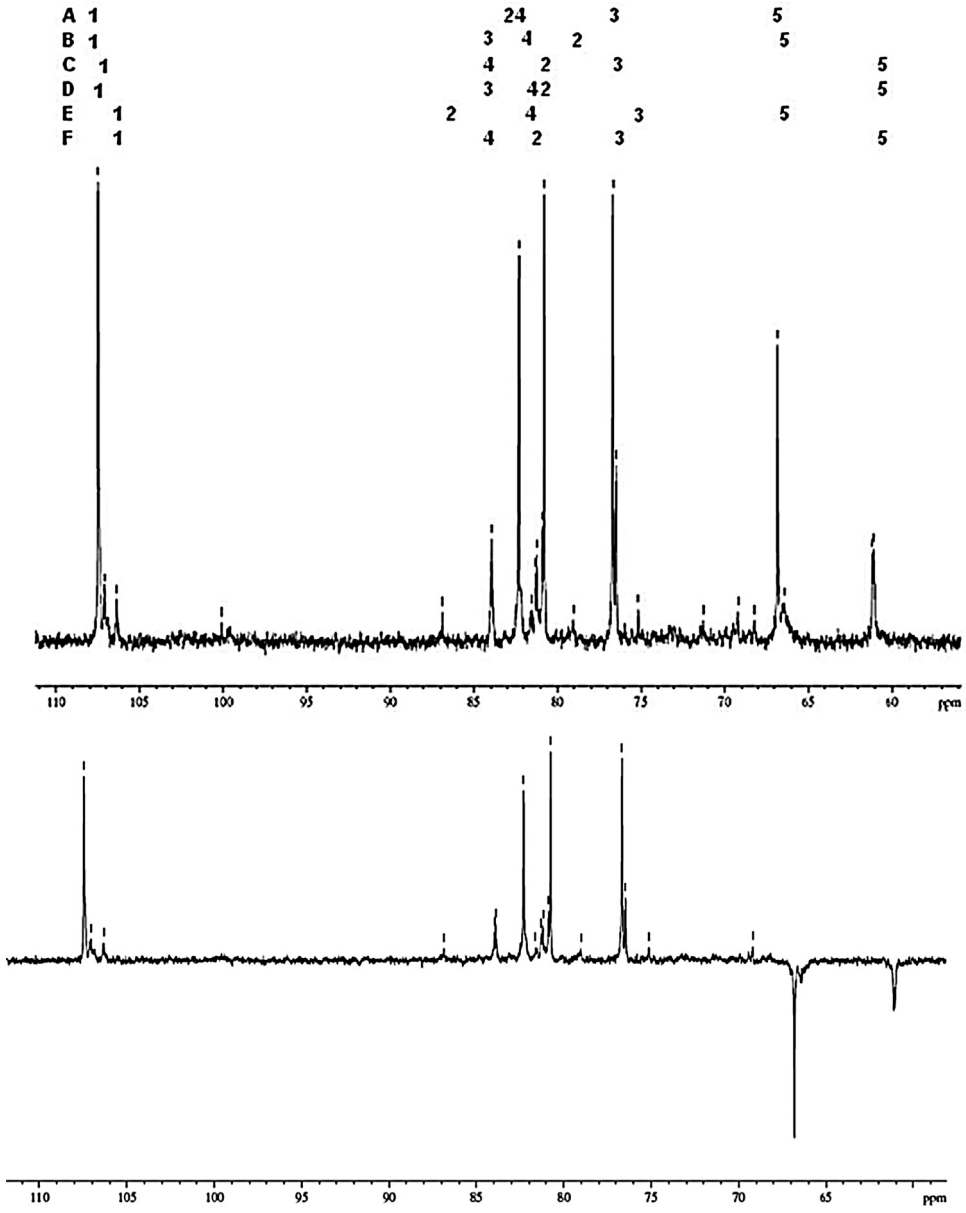

Fig. 3. ^{13}C NMR and DEPT-135 spectrum of ESP-B1H.

Table 2
^{1}H NMR and ^{13}C NMR data of ESP-B1H in D_2O at 400 MHz and 100 MHz.

Glycosyl residues	H-1/C-1	H-2/C-2	H-3/C-3	H-4/C-4	H-5a,H-5b/C-5
→5)-α-Araf-(1→	4.99[a,b,c,d]	4.03[a,b,d]	3.91[a,b,d]	4.12[a,b,d]	3.76–3.82[a,b,c,d], 3.68–3.75[a,b,c,d]
A	107.5[a,c]	82.3[a,c]	76.7[a,c]	82.3[a,c]	66.8[a,c,e]
→3,5)-α-Araf-(1→	5.02[a,b,c,d]	4.20[a,b]	3.98[a,d]	3.92[a]	3.76–3.82[a,b,c], 3.68–3.75[a,b,c,d]
B	107.5[a,c]	79.1[a]	84.0[a,c]	82.0[a,c]	66.4[a,c,e]
α-Araf-(1→	5.06[a,b,c,d]	4.03[a,b]	3.87[a]	4.00[a]	3.70–3.79[a,b,c], 3.60–3.69[a,b,c]
C	107.1[a,c]	80.8[a]	76.5[a,c]	84.0[a,c]	61.1[a,c,e]
→3)-α-Araf-(1→	5.09[a,b,c,d]	4.03[a,b,d]	3.88[a,d]	4.03[a]	3.70–3.79[a,b,c], 3.60–3.69[a,b,c]
D	107.2[a,c]	80.9[a]	84.0[a,c]	81.3[a,c]	61.1[a,c,e]
→2,5)-α-Araf-(1→	5.10[a,b,c,d]	4.07[a,b,d]	4.07[a,d]	4.22	3.76–3.82[a,b,c], 3.68–3.75[a,b,c,d]
E	106.4[a,c]	86.9[a,c]	75.2[a,c]	81.5[a]	66.4[a,c,e]
α-Araf-(1→	5.15[a,b,c]	3.94[a,b]	3.87[a]	3.94[a]	3.70–3.79[a,b,c], 3.60–3.69[a,b,c]
F	106.4[a,c]	81.2[c]	76.5[a]	84.0[a]	61.1[a,c,e]

[a] Assignment from HSQC spectrum.
[b] Assignment from COSY spectrum.
[c] Assignment from HMBC spectrum.
[d] Assignment from NOESY spectrum.
[e] Assignment from DEPT spectrum.

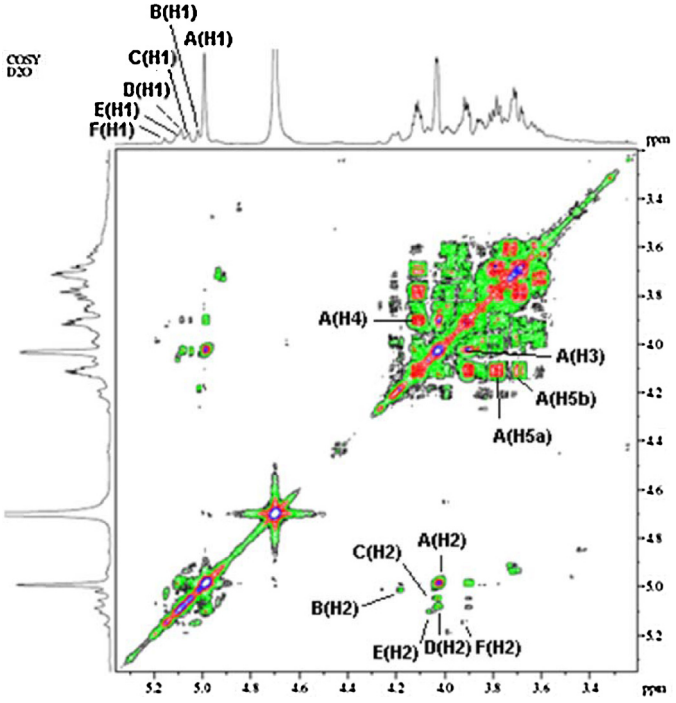

Fig. 4. $^{1}H–^{1}H$ COSY spectrum of ESP-B1H.

(δ_H 4.03) and **A(H3)** (δ_H 3.91), **A(H3)** (δ_H 3.91) and **A(H4)** (δ_H 4.12), **A(H4)** (δ_H 4.12) and **A(H5a** and **5b)** (δ_H 3.76–3.82 and 3.68–3.75); **B(H1)** (δ_H 5.02) and **B(H2)** (δ_H 4.20); **C(H1)** (δ_H 5.06) and **C(H2)** (δ_H 4.03); **D(H1)** (δ_H 5.09) and **D(H2)** (δ_H 4.03); **E(H1)** (δ_H 5.10) and **E(H2)** (δ_H 4.07) and **F(H1)** (δ_H 5.15) and **F(H2)** (δ_H 3.94). These results and the analysis of the HSQC spectrum (Fig. 5) allowed assignment of some carbon signals of the residues **A**-**F**, including carbons **A(C1-C5)** (δ_C 107.5, 82.3, 76.7, 82.3 and 66.8), **B(C1** and **C2)** (δ_C 107.5 and 79.1), **C(C1** and **C2)** (δ_C 107.1 and 80.8), **D(C1** and **C2)** (δ_C 107.2 and 80.9), **E(C1** and **C2)** (δ_C 106.4 and 86.9) and **F(C1** and **C2)** (δ_C 106.4 and 81.2).

We measured the HMBC spectrum to verify the assignments produced by $^{1}H–^{1}H$ COSY and HSQC spectra and to acquire more significant structural information on this arabinan. Examining the cross peaks of both anomeric protons and carbons of each sugar

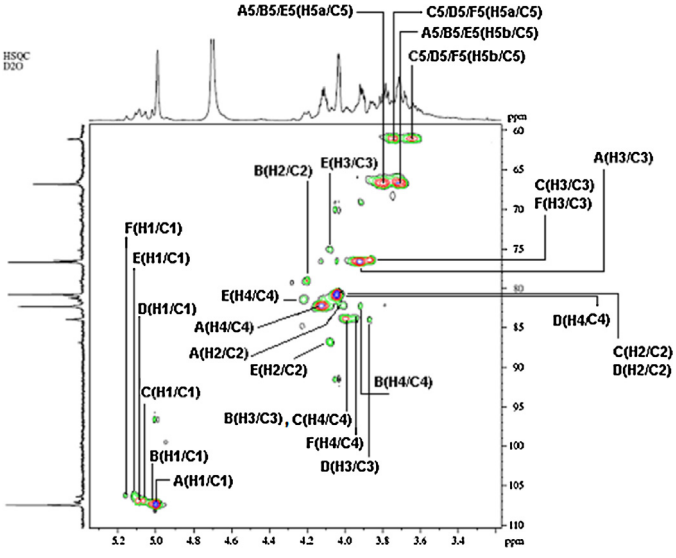

Fig. 5. HSQC spectrum of ESP-B1H.

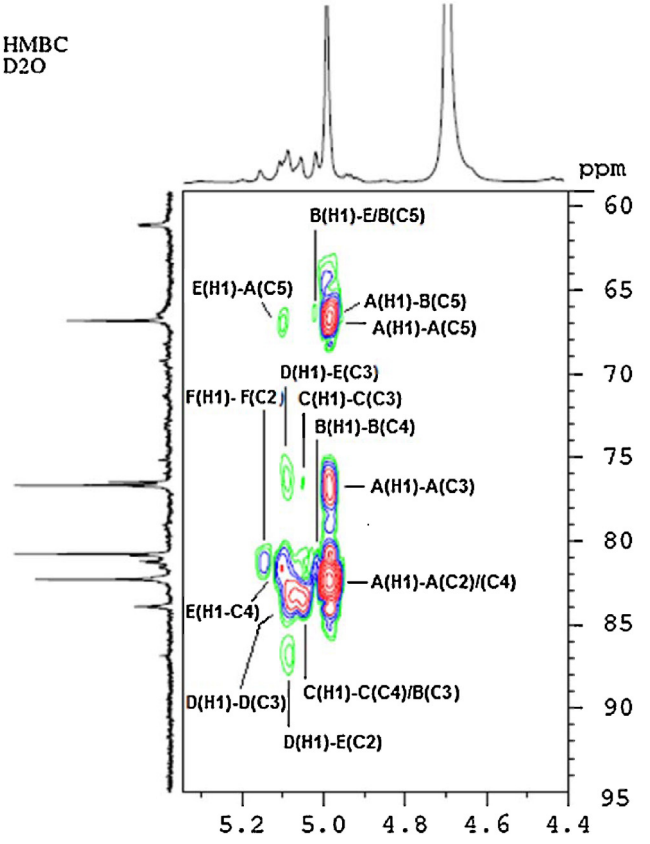

Fig. 6. Key HMBC spectrum of ESP-B1H.

residue in HMBC spectrum, both inter- and intra- residual connectivities were clear (Fig. 6 and Table 3). Some valuable structural information from the anomeric protons was observed through long-range correlations between **A(H1)** (δ_H 4.99) and **A(C5)** (δ_C 66.8) and **B(C5)** (δ_C 66.4) (Sequences **1** and **2**); between **B(H1)**

Table 3
The significant $^{3}J_{H,C}$ connectivities observed in an HMBC spectrum for ESP-B1H.

Residues	Sugar linkages	H-1/C-1 δ_H/δ_C	Observed connectivities		
			δ_H/δ_C	Residues	Atoms
A	→5)-α-Araf-(1→	4.99	66.8	**A**	C-5
		4.99	66.4	**B**	C-5
		4.99	82.3	**A**	C-2
		4.99	76.7	**A**	C-3
		4.99	82.3	**A**	C-4
		107.5	3.76–3.82, 3.68–3.75	**A**	H-5
		107.5	3.76–3.82, 3.68–3.75	**B**	H-5
B	→3,5)-α-Araf-(1→	5.02	66.4	**B**	C-5
		5.02	66.4	**E**	C-5
		5.02	82.0	**B**	C-4
		107.5	3.76–3.82, 3.68–3.75	**B**	H-5
		107.5	3.76–3.82, 3.68–3.75	**E**	H-5
C	α-Araf-(1→	5.06	84.0	**B**	C-3
		5.06	76.5	**C**	C-3
		5.06	84.0	**C**	C-4
D	→3)-α-Araf-(1→	5.09	86.9	**E**	C-2
		5.09	84.0	**D**	C-3
		5.09	75.2	**E**	C-3
E	→2,5)-α-Araf-(1→	5.10	66.8	**A**	C-5
		5.10	81.5	**E**	C-4
F	α-Araf-(1→	5.15	81.2	**F**	C-2

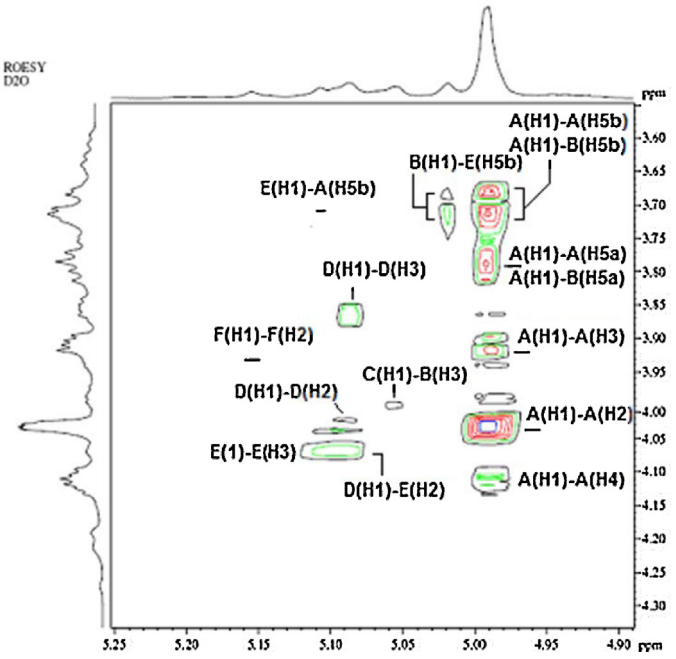

Fig. 7. Part of ROESY spectrum of ESP-B1H.

(δ_H 5.02) and **B(C5)** (δ_C 66.4) and **E(C5)** (δ_C 66.4) (Sequences **3** and **4**); between **C(H1)** (δ_H 5.06) and **B(C3)** (δ_C 84.0) (Sequence **5**); between **D(H1)** (δ_H 5.09) and **E(C2)** (δ_C 86.9), **E(C3)** (δ_C 75.2) and **D(C3)** (δ_C 84.0) (Sequences **6** and **7**); and between **E(H1)** (δ_H 5.10) and **A(C5)** (δ_C 66.8) (Sequence **8**). Note also that the peak outlined in Fig. 6 showed the intra-residual correlations between **A(H1)** (δ_H 4.99) and **A(C2)** (δ_C 82.3), **A(C3)** (δ_C 76.7) and **A(C4)** (δ_C 82.3); between **B(H1)** (δ_H 5.02) and **B(C4)** (δ_C 82.0); between **C(H1)** (δ_H 5.06) and **C(C3)** (δ_C 76.5); and between **E(H1)** (δ_H 5.10) and **E(C4)** (δ_H 81.5). Thus, the following structural sequences **1**–**8** were tentatively deduced. However, structural sequence **9** was deduced because of the good correlation between the terminal and branched α-Ara*f* residues. These assignments reinforce the need to corroborate structural assignments using independent experiments.

Sequence **1**
A **A**
→5)-α-Ara*f*-(1→5)-α-Ara*f*-(1→;
Sequence **2**
A ↓ 3 **B**
→5)-α-Ara*f*-(1→5)-α-Ara*f*-(1→;
Sequence **3**
B ↓ 3 **B**
→3,5)-α-Ara*f*-(1→5)-α-Ara*f*-(1→;
Sequence **4**
B ↓ 2 **E**
→3,5)-α-Ara*f*-(1→5)-α-Ara*f*-(1→;
Sequence **5**
C ↓ 5 **B**
α-Ara*f*-(1→3)-α-Ara*f*-(1→;
Sequence **6**
D ↓ 5 **E**
→3)-α-Ara*f*-(1→2)-α-Ara*f*-(1→;
Sequence **7**
D **D**
→3)-α-Ara*f*-(1→3)-α-Ara*f*-(1→;
Sequence **8**
E **A**
→2,5)-α-Ara*f*-(1→5)-α-Ara*f*-(1→;
Sequence **9**
F **D**
α-Ara*f*-(1→3)-α-Ara*f*-(1→

The ROESY spectrum was used to elucidate the connection of these different structural fragments and confirmed the above assignments. The ROESY experiment (Fig. 7 and Table 4) showed inter-residual contacts between **A(H1)** (δ_H 4.99) and **A(H5b)** (δ_H 3.68–3.75), **B(H5b)** (δ_H 3.68–3.75), **A (H5a)** (δ_H 3.76–3.82) and **B(H5a)** (δ_H 3.76–3.82); between **B(H1)** (δ_H 5.02) and **B(H5b)** (δ_H 3.68–3.75) and **E(H5b)** (δ_H 3.68–3.75); between **C(H1)** (δ_H 5.06) and **B(H3)** (δ_H 3.98); between **D(H1)** (δ_H 5.09) and **D(H3)** (δ_H 3.88) and **E(H2)** (δ_H 4.07); and between **E(H1)** (δ_H 5.10) and **A(H5b)** (δ_H 3.68–3.75). These ROE cross peaks revealed a dipolar interaction, confirming the structures of sequences **1**–**8** proposed. Meanwhile, some intra-residual correlations were also observed between **A(H1)** (δ_H 4.99) and **A(H2)** (δ_H 4.03), **A(H3)** (δ_H 3.91) and **A(H4)** (δ_H 4.12); between **D(H1)** (δ_H 5.09) and **D(H2)** (δ_H 4.03); and between **E(H1)** (δ_H 5.10) and **E(H2/H3)** (δ_H 4.07). The ROESY spectrum showed no intra residual contracts of the residue **C** from H-1 to its own H-5; hence the terminal residue **C** was linked through O-3 to the residue **B**.

Table 4
The significant ROESY data observed in a ROESY spectrum for ESP-B1H.

Anomeric proton		ROE contact protons		
Sugar linkages	δ	δ_H	Residues	Atoms
→5)-α-Ara*f*-(1→	4.99	3.76–3.82	**A**	H-5a
A		3.76–3.82	**B**	H-5a
		3.68–3.75	**A**	H-5b
		3.68–3.75	**B**	H-5b
		4.03	**A**	H-2
		3.91	**A**	H-3
		4.12	**A**	H-4
→3,5)-α-Ara*f*-(1→	5.02	3.68–3.75	**E**	H-5b
B		3.68–3.75	**B**	H-5b
α-Ara*f*-(1→	5.06	3.98	**B**	H-3
C				
→3)-α-Ara*f*-(1→	5.09	3.88	**D**	H-3
D		4.03	**D**	H-2
		4.07	**E**	H-2
→2,5)-α-Ara*f*-(1→	5.10	3.68–3.75	**A**	H-5b
E		4.07	**E**	H-2/H-3
α-Ara*f*-(1→	5.15	3.94	**F**	H-2
F				

Based on the results of monosaccharide composition, methylation analysis and 1D and 2D NMR spectroscopy, the following sequences of ESP-B1H were tentatively determined in Fig. 8. Some possible structures have been predicted due to its characteristically longer (1→5)-α-Ara*f* backbone. It is difficult to identify the accurate structure of this polysaccharide by NMR due to its high molecular weight.

3.4. AFM analysis

AFM has received increasing attention as applied to the study of the surface topography of high molecular polymers and biomacromolecules (Li et al., 1999; Wang et al., 2014; Wu et al., 2009). The 300 μL ESP-B1H solutions were dropped onto freshly cleaved mica and observed by AFM. The planar and cubic AFM images of ESP-B1H were shown in Supplementary Fig. 1. The branched structure of ESP-B1H can be intuitively observed in Supplementary Fig. 1A and B. This result was consistent with the above NMR and GC–MS analysis, which contains branched chains. The height and widths measured for this structure by AFM was about 46.88 nm and 85.94 nm, respectively-values much higher than those of a single polysaccharide chain (about 0.1–1.0 nm). This suggested molecular aggregation (Wang, Sun, Zhang, Chen & Liu, 2012).

Supplementary Fig. 1 related to this article can be found, in the online version, at http://dx.doi.org/10.1016/j.carbpol.2014.12.058.

3.5. Significances of structural elucidation of ESP-B1H

Most arabinans possess a 1,5 linked-α-Ara*f* backbone and arabinofuranosyl branches substituted at O-2 and/or O-3. (Cordeiro et al., 2012; Westphal et al., 2010). A recent report showed that a high molecular weight arabinan ($M_w \sim 2.0 \times 10^5$ Da) contain three T-α-Ara*f* residues inserted in the backbone as branched structures (Mandal et al., 2011). Habibi et al. showed the presence of α-Ara*f*→3)-α-Ara*f*-(1→ attached at O-2 as a branched fragment in the backbone (Habibi, Mahrouz & Vignon, 2005). Another rare arabinan

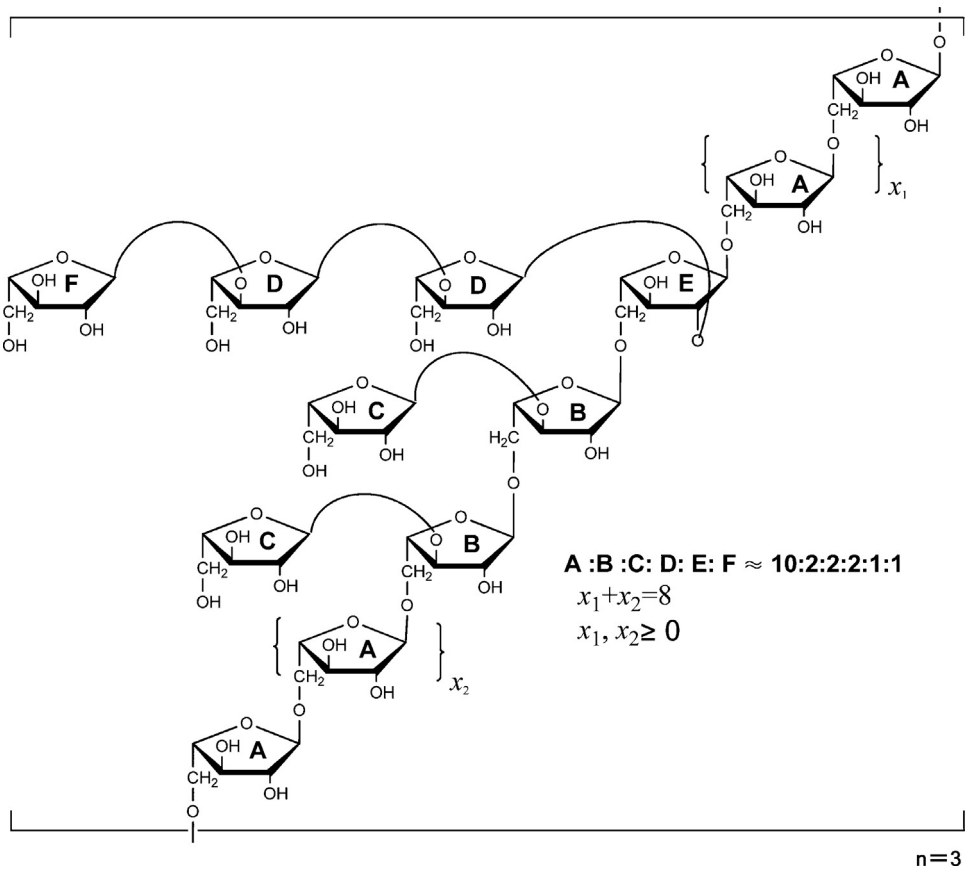

Fig. 8. Tentative structure of ESP-B1H.

isolated from olive pomace was characterized by the presence of a terminal β-Araf (Cardoso et al., 2002). These observations implied extensive structural variation within different arabinans. Although ESP-B1H appeared similar, because it had a 1,5 linked-α-Araf backbone, ESP-B1H has different molecular weights and different molar ratios of sugar residues. This polymer was characterized by a much longer linear (1→5)-α-Araf chain as the backbone. To the best of our knowledge, an α-Araf→3)-α-Araf-(1→3)-α-Araf-(1→ branching at O-2 has not been reported previously.

According to literature, many of the bioactivities of polysaccharides from herb plants are due to their complex branched structures (Kuang et al., 2011a; Sun et al., 2010; Tong, Liang & Wang, 2008). Recently, acidic polysaccharides, extracted from the stem of *E. sinica*, have been confirmed to be an important contributor to immunosuppressive effects. The presence of arabinan and arabinogalactan as structural fragments of *E. sinica* acidic polysaccharides has been shown previously (Kuang et al., 2011a; Kuang et al., 2011b). However, little attention has been given to the branched structures. Therefore, the isolation and identification of this unknown polymeric arabinan would provide essential information for detailed elucidation of the highly complicated structure of *E. sinica* acidic polysaccharides. Furthermore, the elucidation of the molecular structural characteristics of ESP-B1H is quite significant for clarifying the structure–activity relationships of *E. sinica* acidic polysaccharides.

4. Conclusion

Here we describe a new structure of ESP-B1H with a molecular weight of 6.15 kDa from the stems of *E. sinica*. Its complex structure has been tentatively elucidated by methylation analysis combined with GC–MS and 1D and 2D NMR spectroscopic technique. The existence of a branched structure was further observed intuitively by AFM. This is the first report on structural studies of the arabinan from Ephedraceae plants by methylation and 1D and 2D NMR analysis. The current study may facilitate a deeper understanding of chemical structures of *E. sinica* polysaccharides. Further biological studies are necessary to develop carbohydrate-based drugs using these starting materials.

Acknowledgments

This study was partly financially supported by the Major State Basic Research Development Program of China (973 Programs 2013CB531800), National Natural Science Foundation of China (81274103, 30973870 and 81303215), Foundation for the Author of National Excellent Doctoral Dissertation of PR China (201367), Heilongjiang Postdoctoral Foundation (LBH-Q13158 and LBH-Z10019) and Foundation from Heilongjiang University of Chinese Medicine (035094).

References

Cardoso, S. M., Silva, A. M. S., & Coimbra, M. A. (2002). Structural characterisation of the olive pomace pectic polysaccharide arabinan side chains. *Carbohydrate Research*, *337*, 917–924.

Cordeiro, L. M. C., Reinhardt, V. d. F., Baggio, C. H., Werner, M. F. d. P., Burci, L. M., Sassaki, G. L., et al. (2012). Arabinan and arabinan-rich pectic polysaccharides from quinoa (*Chenopodium quinoa*) seeds: Structure and gastroprotective activity. *Food Chemistry*, *130*, 937–944.

Dourado, F., Cardoso, S. M., Silva, A. M. S., Gama, F. M., & Coimbra, M. A. (2006). NMR structural elucidation of the arabinan from *Prunus dulcis* immunobiological active pectic polysaccharides. *Carbohydrate Polymers*, *66*, 27–33.

Dourado, F., Madureira, P., Carvalho, V., Coelho, R., Coimbra, M. A., Vilanova, M., et al. (2004). Purification, structure and immunobiological activity of an arabinan-rich pectic polysaccharide from the cell walls of *Prunus dulcis* seeds. *Carbohydrate Research*, *339*, 2555–2566.

Fernandez, P. V., Quintana, I., Cerezo, A. S., Caramelo, J. J., Pol-Fachin, L., Verli, H., et al. (2013). Anticoagulant activity of a unique sulfated pyranosic (1→3)-beta-L-arabinan through direct interaction with thrombin. *Journal of Biological Chemistry*, *288*, 223–233.

Habibi, Y., Mahrouz, M., & Vignon, M. R. (2005). Arabinan-rich polysaccharides isolated and characterized from the endosperm of the seed of *Opuntia ficus*-indica prickly pear fruits. *Carbohydrate Polymers*, *60*, 319–329.

Kang, J., Cui, S. W., Phillips, G. O., Chen, J., Guo, Q., & Wang, Q. (2011). New studies on gum ghatti (*Anogeissus latifolia*) Part III: Structure characterization of a globular polysaccharide fraction by 1D, 2D NMR spectroscopy and methylation analysis. *Food Hydrocolloids*, *25*, 1999–2007.

Kuang, H., Xia, Y., Yang, B., Wang, Q., & Wang, Y. (2011). Screening and comparison of the immunosuppressive activities of polysaccharides from the stems of *Ephedra sinica* Stapf. *Carbohydrate Polymers*, *83*, 787–795.

Kuang, H., Xia, Y., Liang, J., Yang, B., Wang, Q., & Wang, X. (2011). Structural characteristics of a hyperbranched acidic polysaccharide from the stems of *Ephedra sinica* and its effect on T-cell subsets and their cytokines in DTH mice. *Carbohydrate Polymers*, *86*, 1705–1711.

Kuang, H., Xia, Y., Liang, J., Yang, B., Wang, Q., & Sun, Y. (2011). Fast classification and compositional analysis of polysaccharides from TCMs by ultra-performance liquid chromatography coupled with multivariate analysis. *Carbohydrate Polymers*, *84*, 1258–1266.

Li, H., Rief, M., Oesterhelt, F., Gaub, H. E., Zhang, X., & Shen, J. (1999). Single-molecule force spectroscopy on polysaccharides by AFM-nanomechanical fingerprint of α-(1,4)-linked polysaccharides. *Chemical Physics Letters*, *305*, 197–201.

Mandal, E. K., Mandal, S., Maity, S., Behera, B., Maiti, T. K., & Islam, S. S. (2013). Structural studies of an immunostimulating gluco-arabinan from seeds of *Caesalpinia bonduc*. *Carbohydrate Polymers*, *92*, 704–711.

Mandal, S., Patra, S., Dey, B., Bhunia, S. K., Maity, K. K., & Islam, S. S. (2011). Structural analysis of an arabinan isolated from alkaline extract of the endosperm of seeds of *Caesalpinia bonduc* (*Nata Karanja*). *Carbohydrate Polymers*, *84*, 471–476.

Mehendale, S. R., Bauer, B. A., & Yuan, C. S. (2004). Ephedra-containing dietary supplements in the US versus ephedra as a Chinese medicine. *American Journal of Chinese Medicine*, *32*, 1–10.

Muncey, H. J., Jones, R., De Iorio, M., & Ebbels, T. M. (2010). MetAssimulo: Simulation of realistic NMR metabolic profiles. *BMC Bioinformatics*, *11*, 496.

Navarro, D. A., Cerezo, A. S., & Stortz, C. A. (2002). NMR spectroscopy and chemical studies of an arabinan-rich system from the endosperm of the seed of *Gleditsia triacanthos*. *Carbohydrate Research*, *337*, 255–263.

Shakhmatov, E. G., Toukach, P. V., Michailowa, E. A., & Makarova, E. N. (2014). Structural studies of arabinan-rich pectic polysaccharides from *Abies sibirica* L. Biological activity of pectins of *A. sibirica*. *Carbohydrate Polymers*, *113*, 515–524.

Sun, L., Feng, K., Jiang, R., Chen, J., Zhao, Y., Ma, R., et al. (2010). Water-soluble polysaccharide from *Bupleurum chinense* DC: Isolation, structural features and antioxidant activity. *Carbohydrate Polymers*, *79*, 180–183.

Thude, S., & Classen, B. (2005). High molecular weight constituents from roots of *Echinacea pallida*: An arabinogalactan-protein and an arabinan. *Phytochemistry*, *66*, 1026–1032.

Tong, H., Liang, Z., & Wang, G. (2008). Structural characterization and hypoglycemic activity of a polysaccharide isolated from the fruit of *Physalis alkekengi* L. *Carbohydrate Polymers*, *71*, 316–323.

Uehara, T., Takeshita, M., & Maeda, M. (1992). Studies on anticoagulant-active arabinan sulfates from the green alga *Codium latum*. *Carbohydrate Research*, *235*, 309–311.

Wang, K. P., Wang, J., Li, Q., Zhang, Q., You, R. X., Cheng, Y., et al. (2014). Structural differences and conformational characterization of five bioactive polysaccharides from *Lentinus edodes*. *Food Research International*, *62*, 223–232.

Wang, X. M., Sun, R. G., Zhang, J., Chen, Y. Y., & Liu, N. N. (2012). Structure and antioxidant activity of polysaccharide POJ-U1a extracted by ultrasound from *Ophiopogon japonicus*. *Fitoterapia*, *83*, 1576–1584.

Westphal, Y., Kühnel, S., de Waard, P., Hinz, S. W. A., Schols, H. A., Voragen, A. G. J., et al. (2010). Branched arabino-oligosaccharides isolated from sugar beet arabinan. *Carbohydrate Research*, *345*, 1180–1189.

Wu, J., Deng, X., Zhang, Y., Wang, L., Tian, B.-Q., & Xie, B. J. (2009). Application of atomic force microscopy in the study of polysaccharide. *Agricultural Sciences in China*, *8*, 1458–1465.

Xia, Y. H., Wang, Q. H., Liang, J., Yang, B. Y., Li, G. Y., & Kuang, H. X. (2011). Development and application of a rapid and efficient CZE method coupled with correction factors for determination of monosaccharide composition of acidic heteropolysaccharides from *Ephedra sinica*. *Phytochemical Analysis*, *22*, 103–111.

Xia, Y., Kuang, H., Yang, B., Wang, Q., Liang, J., Sun, Y., et al. (2011). Optimum extraction of acidic polysaccharides from the stems of *Ephedra sinica* Stapf by Box–Behnken statistical design and its anti-complement activity. *Carbohydrate Polymers*, *84*, 282–291.

Yin, J. Y., Lin, H. X., Nie, S. P., Cui, S. W., & Xie, M. Y. (2012). Methylation and 2D NMR analysis of arabinoxylan from the seeds of *Plantago asiatica* L. *Carbohydrate Polymers*, *88*, 1395–1401.